

## Explaining Electromagnetic Induction using the Magnus Effect

Shingo Ito, 5-11-17, Rokkakubashi, Kanagawa Ward, Yokohama City 221-0802, Japan

Correspondence: s-795034@u01.gate01.com

**Abstract:** According to Faraday's formula for electromagnetic induction, the mechanism by which induced electromotive force (EMF) is generated is unclear. This study proposes a possible mechanism by which the induced EMF is generated using a simple experimental setup. Herein, the angle of a circular coil made of copper wire is changed at every 15° (0°–360°) and brought close to the magnetic field at the center of the bar magnet to investigate changes in the EMF. The magnetic force lines are nearly straight and parallel at the center of the bar magnet. Moreover, at this position, the ↑ spin valence electrons are expected to align parallel to the bar magnet's north–south direction. Results showed that EMF varies with the angle and is distributed on the graph of  $y = \sin \theta$ , similar to the Magnus effect of airflow.

**Keywords:** Magnus effect; electromagnetic induction; magnetic flux density; Precession of electrons

### 1. Introduction

Research at the University of Tsukuba [1] has confirmed that ↑ spin electrons in a magnetic field precess clockwise in the direction of the magnetic field. I assumed that since a clockwise top precesses clockwise, electrons rotate clockwise. Therefore, in this research I have assumed that the spin of electrons is clockwise when viewed from the direction of the magnetic field.

This study experimentally verifies whether the relationship between the electron spin and magnetic flux density resembles the relationship between airflow and the Magnus effect [2] shown in Figure 1a when the magnetic flux density is applied at different angles to the electron rotation axis. For the first verification, changes in the Magnus effect were examined by applying air currents at different angles (60°–330°) to a rotating styrene ball. Furthermore, this study investigated whether the electromotive force (EMF) generated when the magnetic flux density at different angles (from 0° to 360°) impinges on the electron's rotation axis is the same as that in the Magnus effect. To this end, all the electrons in the coil should be aligned in the same direction, i.e., the magnetic field lines must be parallel for the electrons to be aligned in the same direction. At magnetic poles, the electrons are not aligned in parallel because the magnetic field lines radiate out from the magnetic pole (Figure 1b); however, if we focus on the magnetic field lines at the center of the bar magnet (Figure 1c), we can see that they are nearly parallel. In this position, I infer that all the valence electrons in the copper circular coil point in the same direction as the magnetic field lines if the coil is at a 90° angle to the bar magnet. Hence, I assumed that the electrons in the coil are not aligned until the coil reaches this position. Therefore, I experimented to measure the (EMF) by fabricating a device in which the coil always enters the magnetic field at the center of the bar magnet at an angle of 90° (Figure 1d). In this device, the bar magnets and coils move at the same angle, which indicates

that the magnetic flux density hits the rotation axis of the electrons at different angles of  $15^\circ$  intervals. Surprisingly, the experimental results were the same as those obtained for the Magnus effect of airflow. Although a simple comparison of the macroscopic rotating ball and microscopic electron spin is difficult, the induced EMF could be due to an interaction between the electron spin and magnetic flux density.

## 2. Materials and Methods

### 2.1. Experiment 1

As depicted in the apparatus shown in Figure 1e, hard steel (with a high elastic modulus) connected to the motor by a coupling was passed through the styrene ball, fixed with an adhesive, and rotated. Then, a scale was used to measure the change in the Magnus effect as airflow hit the center of a rotating ball at different angles of incidence. The airflow hits the rotating styrene ball, the ball is tilted to one side because of the Magnus effect. Here, a scale was used to measure the displacement value of the inclination of the ball. The relational expression between the displacement width  $x$  (mm) of this hard steel wire and cN was  $f(x) = 0.145Ix$ . Furthermore, cN was calculated by substituting the measured displacement into the aforementioned equation. Then, a graph of the Magnus effect for each angle was created. The styrene spheres were selected because they are light; thus, they are easily influenced by the Magnus effect. As shown in Figure 1f, by using coupling, (the device that connects the motor with the rigid wire), the styrene ball (diameter: 50 mm) and the rigid wire forming the rotation axis (diameter: 1.2 mm and length: 398 mm) were connected with a motor. The rotational speed of the styrene ball is 5,925.16 rpm; the wind speed from the blower is 20.4 m/s. A motor (MABUCHI RS-380PH) with a working voltage of 3.3 V was used. The airflow from the blower was applied to the center of the rotating styrene ball, and the displacement width was measured in the range of  $60^\circ$ – $330^\circ$  at an interval of  $15^\circ$ . I averaged the five measurements for each angle of incidence. The measurement range was set from  $60^\circ$  to  $330^\circ$  to prevent the blower from touching the rotating shaft. The rigid wire, protruded from the top of the styrene ball by approximately 3 mm (see “b” in Figure 1f). The maximum value of this displacement was measured using the scale set in front of the styrene ball. To determine the displacement amount of the tilt of the styrene ball, slow-motion shots were captured using an iPad; thereafter, the scale was read while slowly moving at the image.

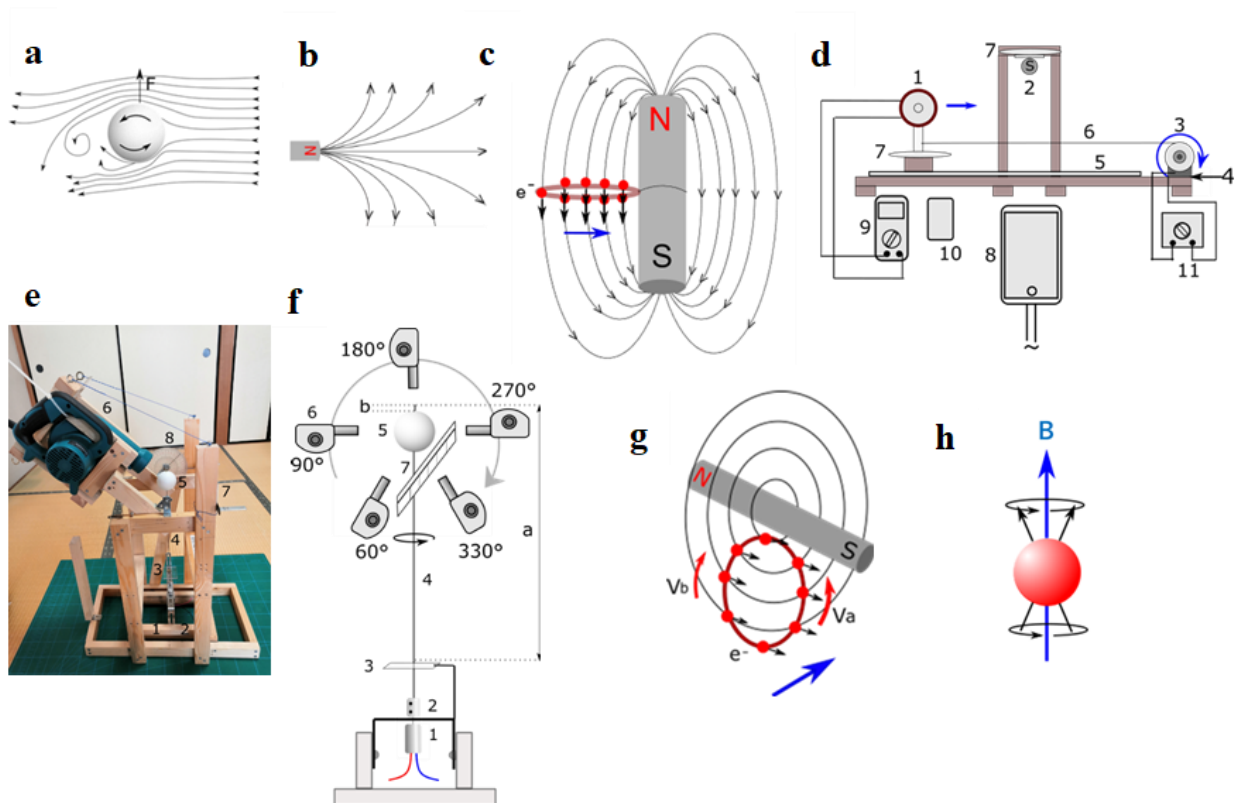


**Figure 1.** Induced electromotive force (EMF) and Magnus effect. **(a)** Magnus effect, **(b)** N pole magnetic field lines **(c)** Red balls, black arrows, and blue arrows indicate electrons in the coil, the direction of electrons, and the direction of the coil motion, respectively. **(d)** Apparatus to measure EMF depending on the incident angle of the coil into the magnetic field. 1: coil, 2: bar magnet, 3: take-up pulley, 4: gearbox with built-in motor, 5: roller stand, 6: kite string, 7: protractor, 8: iPad, 9: digital direct current (DC) voltmeter, 10: smartphone timer, and 11: DC power supply. The distance between right below the center of “2” and the upside center of “1” is 29 mm. **(e)** Equipment for verifying the Magnus effect via airflow. **(f)** Schematic of **(e)**. 1: motor, 2: coupling, 3: support plate, 4: hard steel wire, 5: styrene ball, 6: blower, and 7: scale. In Figure 1e, 8 is a protractor;  $a = 335$  mm and  $b = 3$  mm. **(g)** Red arrows  $V_a$  and  $V_b$  show the EMF generated at the frontside and backside of the coil, respectively. The measured EMF is equal to  $V_a - V_b$ . **(h)** Electrons in precessional motion in a magnetic field.

## 2.2. Experiment 2

The magnetic force lines at the center of the bar magnet were almost parallel and aligned in the same direction (Figure 1c). Therefore, all electrons in the coil were presumed to be aligned in nearly the same direction. Furthermore, as indicated by the blue arrow in Figure 1g, the electrons in the coil proceeding to the center of the bar magnet were considered to generate an upward EMF at this

position (Figure 1g) due to the interaction between the electron spin (rotation) and magnetic flux density. The upward EMF is generated in both the front and end parts. However, as the front part of the coil was closer to the center of the magnet and the magnetic force was stronger, a stronger EMF was considered to be generated there. The EMF measured by the voltmeter corresponded to the difference in the EMFs between the front part of Va and the end part of Vb. Based on these results, a new experimental apparatus (Figure 1d) was constructed. This experimental device allows coils at different angles to pass through the center of a bar magnet. Using this apparatus, the experiments were conducted for  $0^{\circ}$ – $360^{\circ}$  at  $15^{\circ}$  intervals to verify how the EMF changes depending on the incident angle of the coil in the magnetic field. A bar magnet (total length: 110 mm) was prepared by stacking 23 circular neodymium magnets (diameter: 20 mm, thickness: 4.8 mm, and magnetic flux density: 1225 G). The magnetic flux density (G) was 92.2 G at a distance of 37 mm from the center of the bar magnet. The coil used was made by winding a copper wire (diameter, 0.26 mm) 100 times (diameter, 58 mm; coil width, 12 mm; coil thickness,  $\sim 0.5$  mm). The distance from the center of the bar magnet to the center of the top of the coil (a) was 29 mm (Figure 2a). Using a gearbox with a built-in motor, the coil was placed on the roller stand and passed under the center of the bar magnet at a speed of 23.97 mm/s. I used a DC digital voltmeter to measure the EMF (mV) corresponding to the moment the tip of the coil reached just below the center of the bar magnet (Figure 2a). The resolution and accuracy of the voltmeter were 0.1 mV and  $\pm(0.1\% + 1)$ , respectively. I calculated the average value based on 5 measurements for each angle. I found that this digital voltmeter displays the measured value on the LCD display 4 times per second (every 0.25 seconds), so the display is delayed by 0.25 seconds. As a result, measuring the value at 0.25 s after reaching just below the center of the bar magnet was essential. Therefore, using the slow-motion application (SloPro) on the iPad, a video was shot on the same screen using a smartphone timer that can display up to 1/1000 s and a voltmeter. After shooting, the motion on the screen was observed in slow motion; the time at the moment when the tip of the coil reached just below the center of the bar magnet was confirmed using a timer, and the value (mV) of the voltmeter was read 0.25 s later. Both the bar magnet and circular coil could rotate  $360^{\circ}$  and a protractor was set at each instrument to confirm the angle. As shown in Figures 2b1, b2, and b3, which are top views of Figure 1d, the voltmeter value (mV) was always measured 0.25 s after the moment the coil entered the magnetic field of the bar magnet at right angles, with the coil and bar magnet adjusted at the same angle. The measured angle range was  $0^{\circ}$ – $360^{\circ}$ ; I measured the EMF every  $15^{\circ}$ . The measurement timing is when the tip of the coil reaches just below the center of the bar magnet and the coil becomes perpendicular to the bar magnet. (Figure 2c). It is expected that the electrons in the coil were always aligned in the same direction, as indicated by the red arrow, due to the magnetic field at this position. Accordingly, the electrons in the coil were aligned on a straight line (“a” in Figure 2c) and facing the same direction, and all electrons were subjected to the motion of

the magnetic flux density, as indicated by the black arrow from the same direction. I believe that this would cause an upward EMF similar to the Magnus effect of air currents. The main body, various mounting fixtures, screws, and nuts were made of wood, aluminum, and brass. Although these materials do not affect the magnetic field, the roller stand shown in Figure 1d (5) was made of iron. However, since the bar magnet is far away from the roller stand, I thought the effect would be minimal.

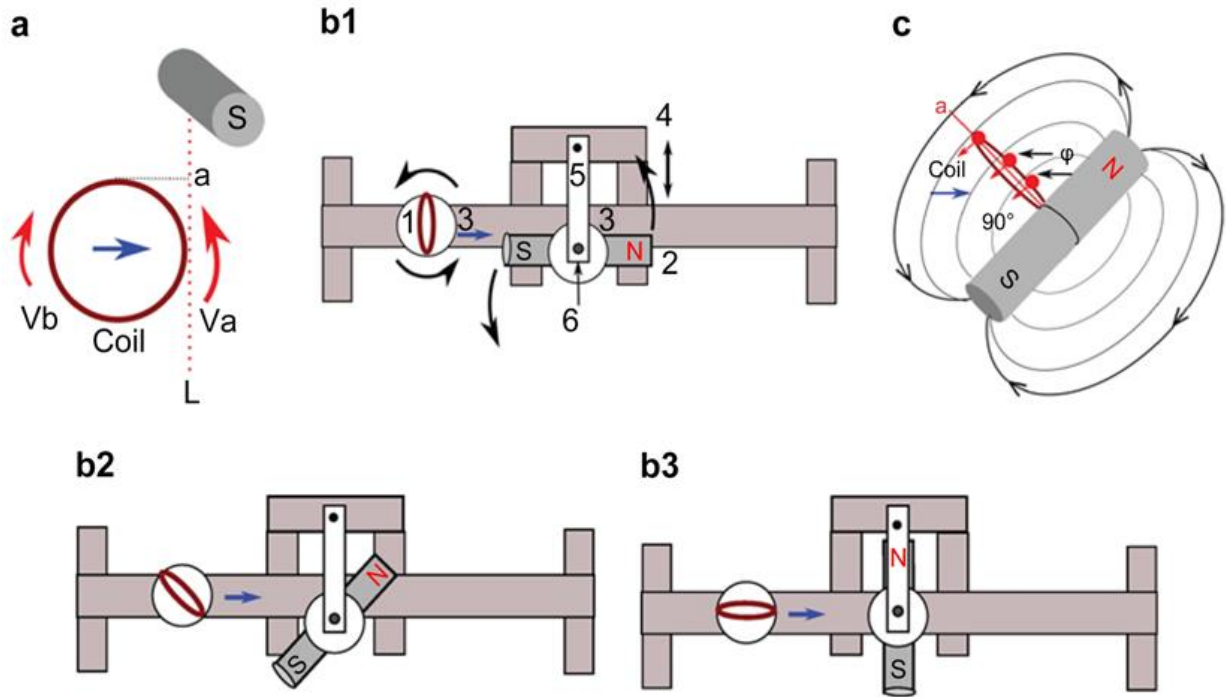


**Figure 2.** Angle of the coil proceeding toward the magnetic field and the angle of the magnet. (a) Measurement position of the EMF of the coil. (b) Top view of Figure 1d with 1: coil, 2: bar magnet, 3: protractor, 4: magnet mounting base movable, 5: aluminum fitting, 6: screw, and the blue arrow representing coil movement. b1: coil entering at  $0^\circ$ , b2: coil entering at  $45^\circ$ , and b3: coil entering at  $90^\circ$ . (c) The red balls, red arrows, black arrows, and blue arrows show the electrons within the coil, the direction of electrons, the direction of magnetic flux density, and coil motion, respectively.

### 3. Results

#### 3.1. Experiment 1

Table 1 shows the Magnus effect data for each angle obtained in Experiment 1. Figure 3a shows a graph obtained by dividing the value obtained this way using the value 2.1185 at  $90^\circ$ . The solid line represents the graph for  $y = \sin\theta$ . The Magnus effect peaks at  $90^\circ$  (Figure 1f); however, at  $180^\circ$ , i.e., directly above the Styrofoam ball, it is nearly zero. Beyond that position, the Magnus effect begins to reverse and the displacement reaches a maximum at  $270^\circ$ .

**Table 1.** Data of Magnus effect due to airflow for each angle.

| Angle | Displacement<br>(mm) | cN      | With 90° as 1 |
|-------|----------------------|---------|---------------|
| 60    | 11.0                 | 1.5961  | 0.7534        |
| 75    | 13.8                 | 2.0024  | 0.9452        |
| 90    | 14.6                 | 2.1185  | 1.0000        |
| 105   | 14.2                 | 2.0604  | 0.9726        |
| 120   | 11.6                 | 1.6832  | 0.7945        |
| 135   | 9.2                  | 1.3349  | 0.6301        |
| 150   | 6.9                  | 1.0012  | 0.4726        |
| 165   | 4.8                  | 0.6965  | 0.3288        |
| 180   | 0.7                  | 0.1016  | 0.0480        |
| 195   | -4.7                 | -0.6820 | -0.3219       |
| 210   | -7.0                 | -1.0157 | -0.4794       |
| 225   | -10.2                | -1.4800 | -0.6986       |
| 240   | -12.4                | -1.7992 | -0.8493       |
| 255   | -14.4                | -2.0894 | -0.9863       |
| 270   | -14.6                | -2.1185 | -1.0000       |
| 285   | -13.6                | -1.9734 | -0.9315       |
| 300   | -12.4                | -1.7992 | -0.8493       |
| 315   | -10.2                | -1.4800 | -0.6986       |
| 330   | -6.6                 | -0.9577 | -0.4521       |

### 3.2. Experiment 2

Table 2 shows the EMF (mV) data for each angle obtained from Experiment 2. Figure 3b shows a graph obtained by dividing the value obtained this way using the value 0.348 at 90°. The solid line is the graph of  $y = \sin\theta$ . The EMF was almost zero at 0°, maximum at 90°, and almost zero again at 180°. Thereafter, the values became negative, reaching a maximum at 270° and almost 0 at 360°.

**Table 2.** Experimental data of the EMF at each angle at the center of the bar magnet.

| Angle | Electromotive<br>force<br>(mV) | With 90° as 1 | Angle | Electromotive<br>force<br>(mV) | With 90° as 1 |
|-------|--------------------------------|---------------|-------|--------------------------------|---------------|
| 0     | 0.004                          | 0.011         | 195   | -0.086                         | -0.247        |
| 15    | 0.112                          | 0.322         | 210   | -0.168                         | -0.483        |
| 30    | 0.176                          | 0.506         | 225   | -0.252                         | -0.724        |
| 45    | 0.230                          | 0.661         | 240   | -0.290                         | -0.833        |
| 60    | 0.320                          | 0.920         | 255   | -0.326                         | -0.937        |
| 75    | 0.330                          | 0.948         | 270   | -0.334                         | -0.960        |
| 90    | 0.348                          | 1.000         | 285   | -0.300                         | -0.862        |
| 105   | 0.338                          | 0.971         | 300   | -0.286                         | -0.822        |
| 120   | 0.320                          | 0.920         | 315   | -0.220                         | -0.632        |
| 135   | 0.218                          | 0.626         | 330   | -0.138                         | -0.397        |
| 150   | 0.172                          | 0.494         | 345   | -0.040                         | -0.115        |
| 165   | 0.066                          | 0.190         | 360   | 0.026                          | 0.075         |
| 180   | 0.010                          | 0.029         |       |                                |               |

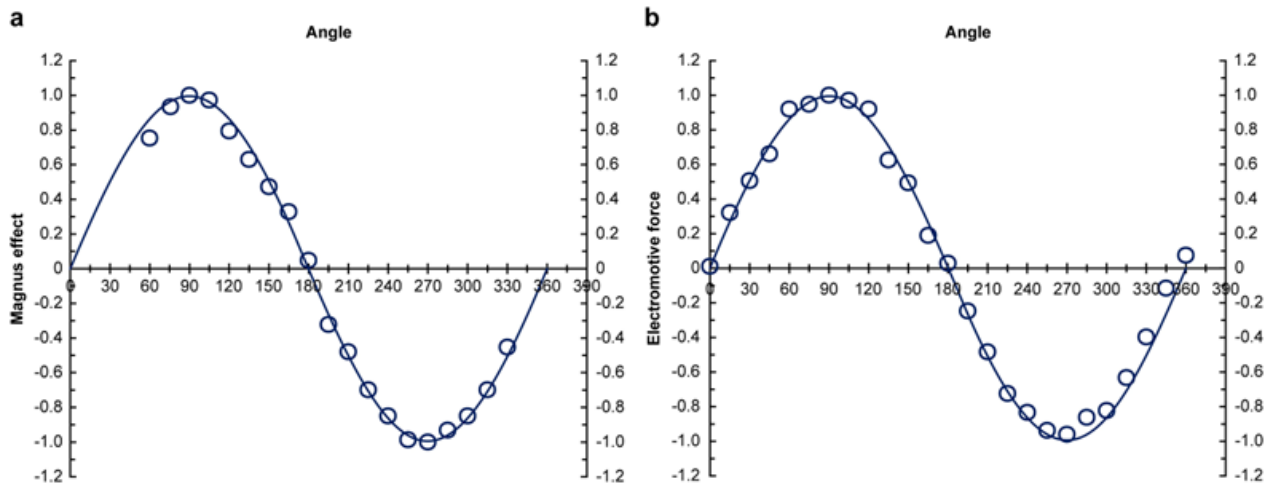


**Figure 3.** Graphs from experimental data. (a) Magnus effect due to air flow at each angle. The open circles show the values where the measured values were divided by that at  $90^\circ$ . The solid line shows the graph represented as  $y = \sin\theta$ . (b) EMF at the center of the bar magnet at each angle. The open circles show the values where the EMF at each angle was divided by the value at  $90^\circ$ . The solid line shows the graph represented as  $y = \sin\theta$ .

#### 4. Discussion

The Magnus effects due to air flow at each angle (Experiment 1) were distributed on the graph of  $y = \sin\theta$  in the range of  $60^\circ$ – $330^\circ$  (Figure 3a). Furthermore, the EMF in the central part of the bar magnet at each angle seems distributed on the graph of  $y = \sin\theta$  in the  $0^\circ$ – $360^\circ$  range (Figure 3b). These results indicate that when airflow hits a rotating sphere and also when a magnetic flux density hits a spinning (rotating) electron, the same mechanism works. The results described so far show that when airflow hits the rotating sphere by changing the incident angle against the rotation axis of the sphere, the Magnus effect changes. Furthermore, the EMF changes when a magnetic flux density with a different incident angle hits the rotation axis of a spinning (rotating) electron. These phenomena can be explained based on Figure 4a, in which the black arrows represent the magnitude of the magnetic flux density at each incident angle against the electron. Even when the incident angle is different, all the magnitudes of the magnetic flux density are equal because the speed of the coil is the same. The bold red arrows, which show the direction of electrons, indicate that the direction of the electrons is toward the right, i.e., the direction of the magnetic field. Considering that the electrons rotate clockwise relative to the direction of the magnetic field, EMF is considered to be generated via the phenomenon estimated to be the Magnus effect in the forward direction, as shown by the blue arrow. The EMF generated by the phenomenon estimated to be the Magnus effect becomes largest when the magnetic flux density hits the rotation axis of the electron at  $90^\circ$ .

The phenomenon that can be speculated as the Magnus effect seems to be related to the component striking at  $90^\circ$  to the electron rotation axis. Each red arrow in a, b, c, and d represents the magnitude of the magnetic flux density of the component that hits the electron rotation axis at  $90^\circ$  (downward in Figure 4a). The magnitude of the magnetic flux density is the largest at  $90^\circ$  for “a,” and it is expected to be the smallest at  $0^\circ$  for “d.” Additionally, the magnitude is expected to be expressed by  $\sin\theta$ . When the magnitude of a magnetic flux density that hits an electron is attenuated according to  $\sin\theta$ , the EMF can also be assumed attenuated according to its ratio. Therefore, the changes in the EMF of electrons are estimated to be distributed on the graph of  $y = \sin\theta$ , similar to changes in the Magnus effect for airflow.

Furthermore, it can be inferred that this phenomenon is the Magnus effect due to magnetic flux density acting on the axis of rotation of the electron, and therefore follows Fleming's right-hand rule.

Comparing Figures 4b and 4c, these two cases are estimated to represent the same phenomena. When the electron aligns in the direction of the magnetic field and when it is rotating clockwise by looking toward this direction, the magnetic flux density moves relatively downward according to the upward motion of the coil (conductor) (Figure 4b). At that moment, EMF is generated via the Magnus effect, and electrons move backward. Because the electric current is reversed with respect to the motion of electrons, the current flows to the front. Based on these considerations, the phenomenon estimated to be the Magnus effect of electrons can also be considered to be expressed by Fleming's right-hand law (Figure 4c). Further, we considered whether the Lorentz force acting on electrons moving in a magnetic field can be explained by the phenomenon estimated to be the Magnus effect of electrons. Let us compare Figure 4d with Figure 4e. Let the electron in Figure 4d move in the direction of the back in the magnetic field pointing to the right side. Because the electric current is reversed with respect to the motion of electrons, the current flows to the front. The thin black arrows pointing to the right represent the magnetic field direction. The electron will change its trajectory by receiving the upward Lorentz force. This Lorentz force is presented in Figure 4e, i.e., Fleming's left-hand law. Because the electron in Figure 4d is moving backward, the magnetic flux density relatively moves to the front, as shown by the thin blue arrows. If the electron is rotating clockwise with respect to the magnetic field direction, the electron will gain the upward force via the phenomenon estimated to be the Magnus effect of this moving magnetic flux density. Therefore, both the Lorentz force and Fleming's left-hand law could be explained by the phenomenon estimated to be the Magnus effect of the electron rotation and moving magnetic flux density.



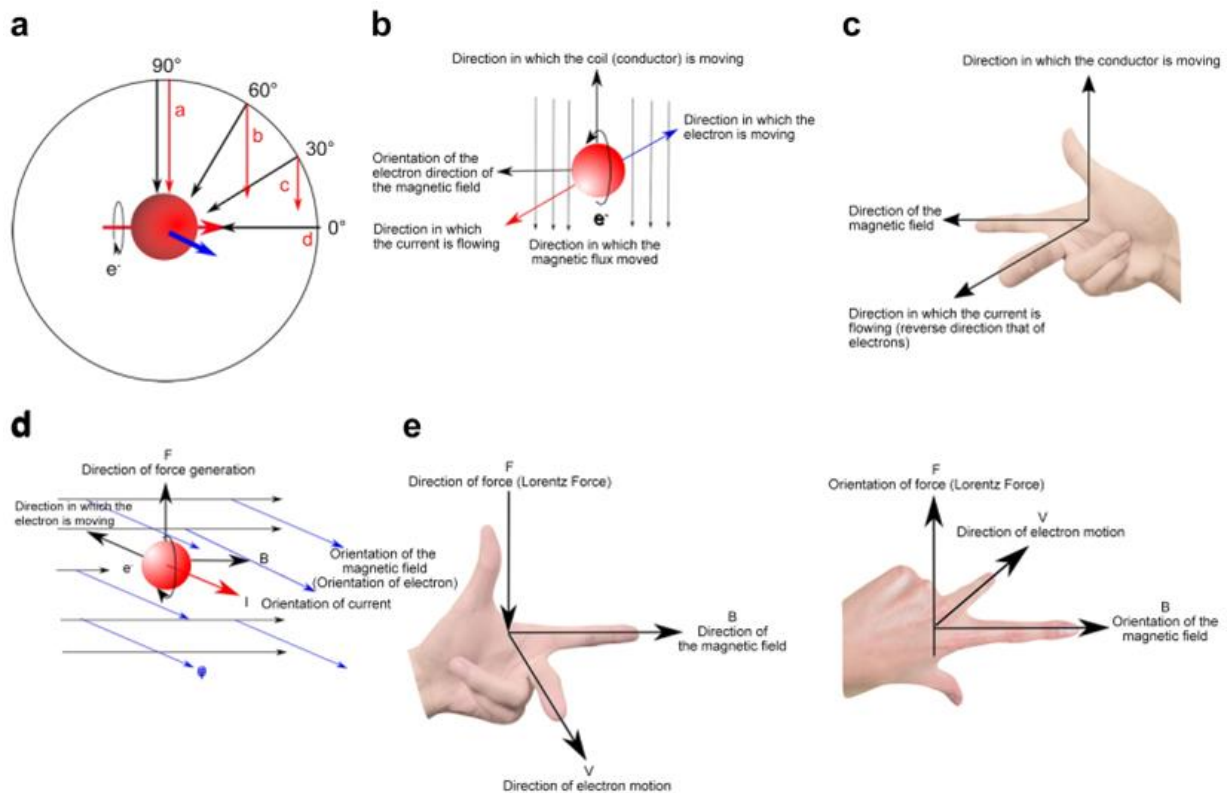


**Figure 4.** Contrasting the Magnus effect and the movement of electrons. **(a)** Change in the EMF of electrons. **(b)** The direction of electron motion when the coil moves in the magnetic field. The red ball is a precessing electron. The black arrow in the upward direction indicates the direction in which the coil is moving. The black arrow in the left direction is the direction of the magnetic field. The thin black arrow pointing downward is the direction in which the magnetic flux density is moving. The blue arrow indicates the direction in which the electron is moving. **(c)** Fleming's right-hand law. **(d)** The red ball is the spinning electron. The black arrow in the back direction is the direction in which the electron is moving. The black arrow in the right direction is the direction of the magnetic field. The blue arrow pointing front side represents the movement of the magnetic flux density. The black arrows in the upper direction show the orientation of force. **(e)** Fleming's left-hand law (in cases of the electron) at the front and back.

## 5. Conclusions

Collectively, the results indicate that the EMF generated in the coil moving in the magnetic field is caused by the Magnus effect, which is the interaction between a rotating electron and the magnetic flux density hitting it. Yoshida et al. [1] observed that the electron precesses clockwise when viewed from the magnetic field's direction. Based on this observation, I have been working on the assumption that the electrons are rotating clockwise because the clockwise spinning top is

precessing clockwise. Modern quantum physics does not consider electron spin to be rotation. However, I can explain this phenomenon by assuming that it is the rotation of electrons. Anyone can easily make this experimental device and conduct experiments, so I would like researchers to replicate this experiment and confirm that the published data is correct. Furthermore, as the experimental equipment used in this study cannot measure changes in the flow of magnetic flux density, precise experimental equipment should be used in the future to confirm whether the EMF is generated by the pressure difference in the magnetic flux density when the magnetic flux density hits the rotating electrons, as in my consideration.

**Author Contribution:** Conceptualization, S.I.; methodology, S.I.; formal analysis, S.I.; data curation, S.I.

**Funding:** This research received no external funding.

**Institutional Review Board Statement:** Not applicable.

**Informed Consent Statement:** Not applicable.

**Data Availability Statement:** The datasets generated and/or analyzed during the current study are available from the corresponding author upon reasonable request.

**Conflicts of Interest:** The author declares no conflict of interest.

## References

1. Yoshida, S.; Aizawa, Y.; Wang, Z.H.; Oshima, R.; Mera, Y.; Matsuyama, E.; Oigawa, H.; Takeuchi, O; Shigekawa, H. Probing ultrafast spin dynamics with optical pump-probe scanning tunneling microscopy. *Nature Nanotechnology* **2014**, *9*, 588–593.

University of Tsukuba paper (Japanese)

<https://www.tsukuba.ac.jp/images/92a9444fccb085f99705b353bb27a6cd.pdf>

2. Muto, M.; Watanabe, H.; Tsubokura, M.; Oshima, N. Negative Magnus effect on a rotating sphere at around the critical Reynolds number. *J. Phys. Conf. Ser* **2011**, *318*, 032021.